Article

Crystal Structure and Electrical Characteristics of (0.965)(Li$_{0.03}$(Na$_{0.5}$K$_{0.5}$)0.97)(Nb$_{1−x}$Sb$_x$)O$_3$−0.035(Bi$_{0.5}$Na$_{0.5}$)$_{0.9}$(Sr)$_{0.1}$ZrO$_3$ Ceramics Doped with CuO, B$_2$O$_3$, and ZnO

Juhyun Yoo * and Sujin Kang

Department of Electrical Engineering, Semyung University, Jecheon 390-711, Korea; sujin95k@nate.com
* Correspondence: juhyun57@semyung.ac.kr; Tel.: +82-43-649-1301; Fax: +82-43-643-0868

Abstract: Recently, the need has arisen to enhance the piezoelectric properties and temperature stability of (Na,K)NbO$_3$ system ceramics. The (0.965)(Li$_{0.03}$(Na$_{0.5}$K$_{0.5}$)0.97)(Nb$_{1−x}$Sb$_x$)O$_3$−0.035(Bi$_{0.5}$Na$_{0.5}$)$_{0.9}$(Sr)$_{0.1}$ZrO$_3$ ceramics were newly manufactured using the sintering aids of CuO, B$_2$O$_3$, and ZnO as a function of antimony substitution, and the their crystal structure and electrical characteristics were analyzed. The grain size was apparently refined as the amount of antimony increased. The dielectric constant was enhanced and Curie temperature was decreased due to the content of the antimony substitution. The x = 0.07 sample sintered at 1060 °C presented the best electrical characteristics, which were bulk density = 4.488 g/cm^3, piezoelectric constant d$_{33}$ = 330 pC/N, electromechanical coupling factor k$_p$ = 0.427, mechanical coupling factor Q$_m$ = 61, and dielectric constant ε$_r$ = 2521. We believe that the x = 0.07 sample is the best material for piezoelectric speakers.

Keywords: crystal structure; electrical characteristics; d$_{33}$; antimony; Curie temperature

1. Introduction

In recent years, lead zirconate titanate ceramics have been extensively utilized in application devices such as piezoelectric actuator, ultrasonic motors, piezoelectric transformer, and ultrasonic cutters [1–5]. In particular, various multi-structured piezoelectric ceramics were investigated for the application of piezoelectric speaker capable of being used in smart phone speaker. It is well known that (Bi$_{0.5}$Na$_{0.5}$)ZrO$_3$ addition could simultaneously increase TR-O(Rhombohedral-Orthorhombic transition temperature) and decrease TO-T (Orthorhombic-tetragonal transition temperature) of KNN ((K,Na)NbO$_3$) system ceramics. Accordingly, a rhombohedral-tetragonal (R-T) coexistence phase can appear. Because this R-T phase transition may act similarly to the classical morphotropic phase boundary (MPB) observed in PZT ceramics, the higher d$_{33}$ may be expected [6–13]. Therefore, in compositionally modified KNN ceramics, increased dielectric and piezoelectric properties can be obtained by forming the R-T Polymorphic phase transition (PPT) near room temperature. It is well-known that the MPB region with tetragonal and rhombohedral structure can enhance the piezoelectricity of the PZT ceramics, owing to the involvement of the more polarization states [14]. Accordingly, piezoelectric devices have mainly utilized the ceramics close to the tetragonal and rhombohedral phase boundary.

The predominant KNN system ceramics substituted with (Ba,Na)ZrO$_3$ were developed due to the coexistence of tetragonal and rhombohedral phases [15].
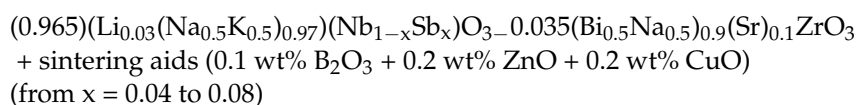
The KNN system ceramics have sintered at a high sintering temperature of more than 1100 °C. Accordingly, the ceramics can induce compositional fluctuation owing to rapid volatilization of alkali elements at above 1100 °C [16]. Moreover, cheap Ag rich-Pd inner electrode in the multilayer structured ceramics should be used for price competitiveness. CuO, B$_2$O$_3$, and ZnO can also be utilized as the sintering aids in order to decrease the sintering temperature of the KNN ceramics. A low temperature sintering process for the ceramics can be achieved using the liquid phase formation owing to their lower melting

point. Antimony (Sb) substituted with the KNN system can also decrease $T_{O\text{-}T}$ and increase $T_{R\text{-}O}$ [17,18]. The increase of piezoelectric ceramic strain (S) according to the electric field (E) can enhance the sound pressure level of the piezoelectric speaker ($S = d_{33}E$). Accordingly, with the aim of enhancing the piezoelectric constant d_{33}, physical properties, and temperature stability of $(Na,K)NbO_3$ ceramics, $(0.965)(Li_{0.03}(Na_{0.5}K_{0.5})_{0.97})$

$(Nb_{1-x}Sb_x)O_{3-}0.035(Bi_{0.5}Na_{0.5})_{0.9}(Sr)_{0.1}ZrO_3$ ceramics were newly manufactured using the sintering aids of CuO, B_2O_3, and ZnO as a function of antimony substitution. Here, we have selected the x = 0.04–0.08 composition ceramics to focus on the composition of R-T MPB regions, and their crystal structure and electrical characteristics were investigated for piezoelectric speaker applications.

2. Experiments

In these experiments, the following composition samples were fabricated according to the following traditional manufacturing method [19];

$(0.965)(Li_{0.03}(Na_{0.5}K_{0.5})_{0.97})(Nb_{1-x}Sb_x)O_{3-}0.035(Bi_{0.5}Na_{0.5})_{0.9}(Sr)_{0.1}ZrO_3$
+ sintering aids (0.1 wt% B_2O_3 + 0.2 wt% ZnO + 0.2 wt% CuO)
(from x = 0.04 to 0.08)

All raw materials, including K_2CO_3, Li_2CO_3, Na_2CO_3, Sb_2O_5, $SrCO_3$, Bi_2O_3, and ZrO_2, were ball-milled for 24 h, and the powders were dried and calcined at 850 °C for 6 h. After performing calcining, CuO, B_2O_3, and ZnO as the sintering aids were added, and then, a PVA as binder was added to the dried powders. The powders including the binder were formed by a pressure of 17 MPa using a mold with a diameter of 17 mm, and then the ceramics formed were sintered at 1060 °C for 10 h. The density was measured using the Archimedes method. For the purpose of measuring the electrical characteristics, all samples lapped to thickness (= 1.0 mm) were electro-deposited using Ag paste. In order to measure the piezoelectric and dielectric characteristics, the specimens were polished to 1 mm thickness and then electrodeposited with Ag paste. Poling of the samples was carried out at 120 °C in a silicon oil bath by applying DC fields of 3 kV/mm for 30 min. To investigate the dielectric properties, capacitance was measured at 1 kHz (standard frequency) using an LCR meter (ANDO AG-4034) (Rancho Cordova, CA, USA) and the dielectric constant of the non-poled sample was calculated. Piezoelectric constants were obtained using a d_{33} meter (APC-90-2030, 46 Heckman Gap Road, Mill Hall, PA 17751, USA). To investigate the piezoelectric properties, the resonant and anti-resonant frequencies were measured using an Impedance Analyzer (Agilent 4294A, 1150 Raymond Avenue SW Renton, WA, USA) according to IRE standard, and then the electromechanical coupling factor k_p and mechanical quality factor Qm were calculated [20].

To determine the crystal structure of the specimen, the X-ray diffraction meter (XRD: Rigaku, D/MAX-2500H) was irradiated at a diffraction angle 2θ between 20° and 80° by a powder method using a CuKα line having a wavelength of λ = 1.5406 Å. The microstructure of the specimen was observed at 3000 magnification with the aids of a scanning electron microscope (SEM: Model Hitachi, S-2400) [17,18].

3. Results and Discussion

The microstructure of samples with antimony are shown in Figure 1. The surface grain size of the samples were significantly reduced with the increase of the antimony. This is explained by the fact that the Sb^{5+} ion can reduce the average grain size with the increase of antimony [19,20]. As shown in Figure 2, the grain size was refined as the amount of Sb^{5+} further increased from 5.2 μm (x = 0.04) to 2.3 μm (x = 0.08) [20]. According to the decrease of grain size, densification of the crystal microstructure was also performed. Sintering aids CuO, B_2O_3, and ZnO may promote the chemical reaction of ceramic particles owing to a liquid phase formation and then can enhance the ceramic densification.
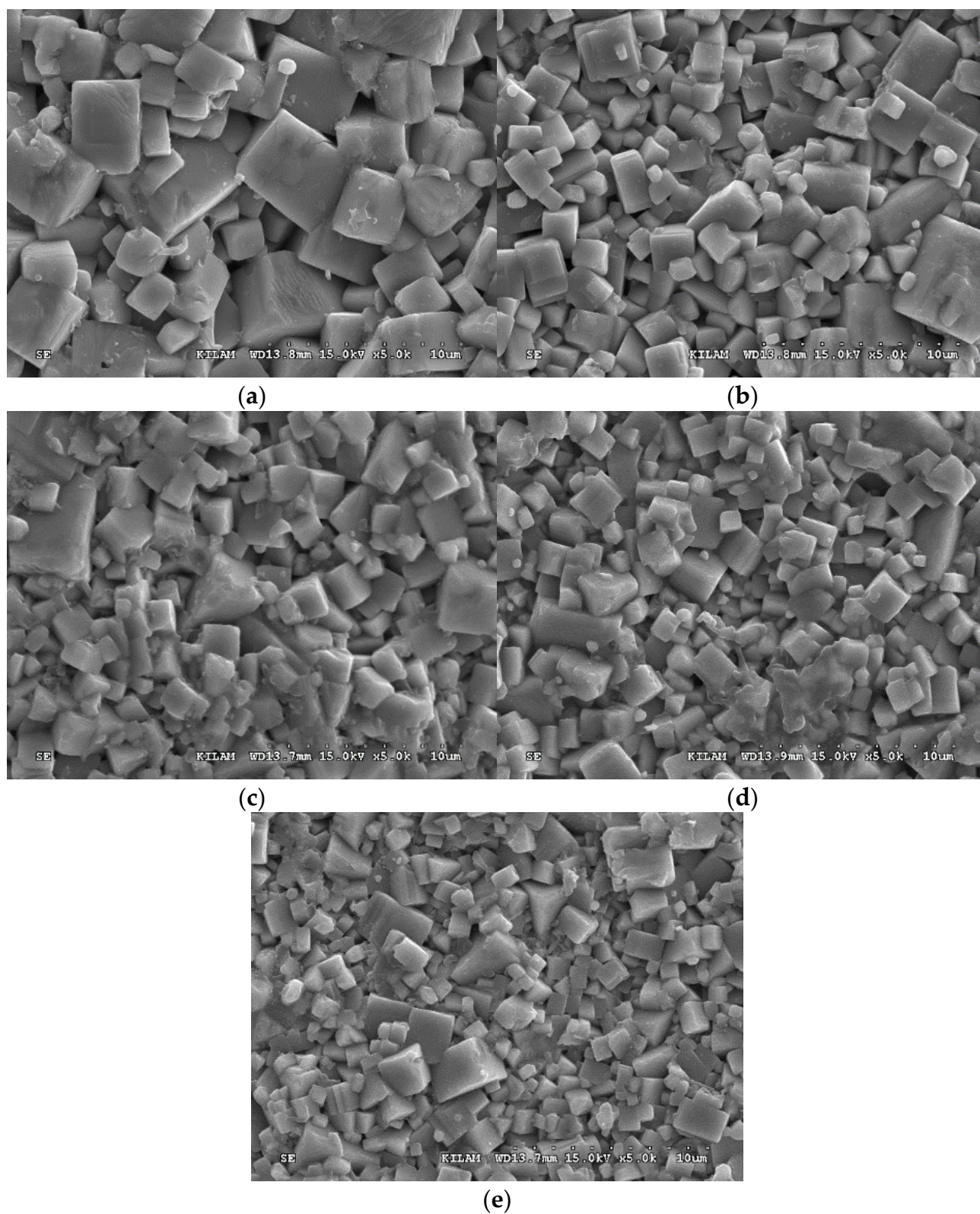
Figure 1. Scanning electron microscopy (SEM) of samples with the amount of antimony (**a**) x = 0.04, (**b**) x = 0.05, (**c**) x = 0.06, (**d**) x = 0.07, (**e**) x = 0.08.
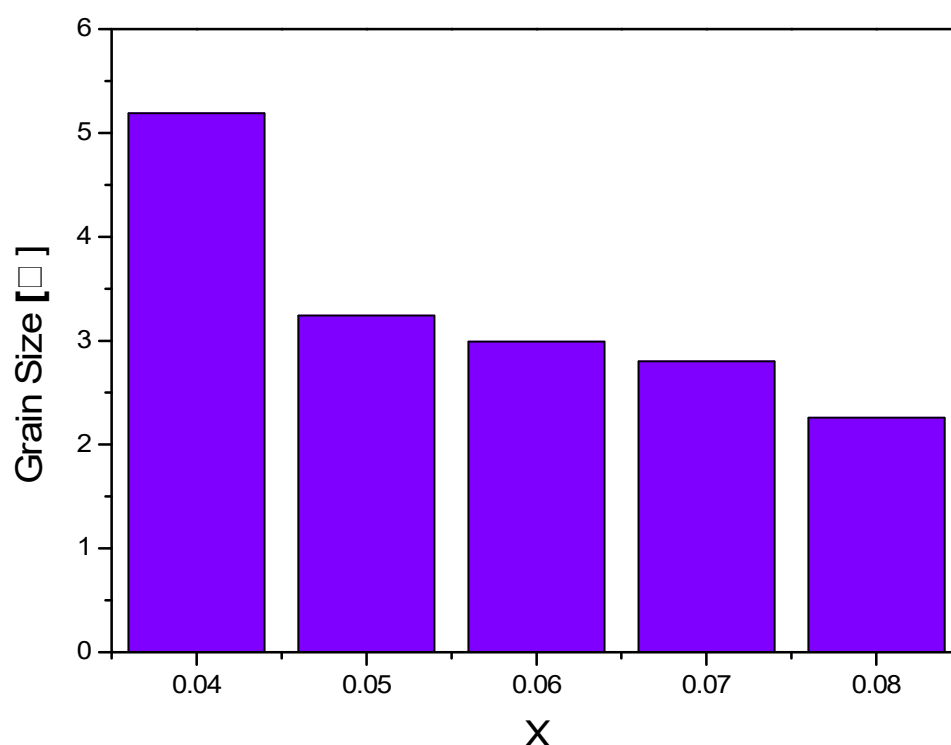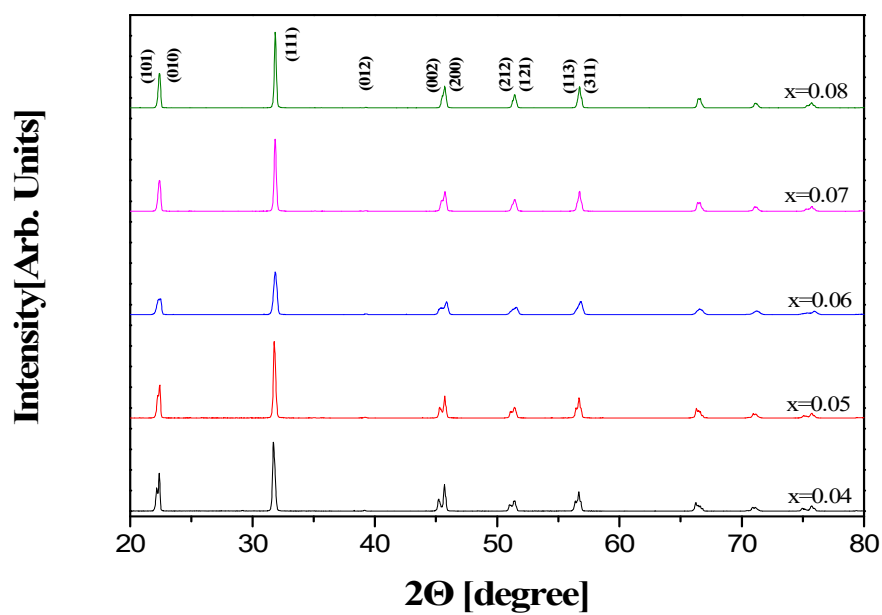
Figure 2. Grain size of samples with the amount of antimony.

The X-ray diffraction (XRD) pattern with the antimony of samples fired at 1060 °C for 10 h are shown in Figure 3. All off the samples exhibit pure perovskite phase, and no secondary phases were investigated. The ceramic samples from x = 0.04 to x = 0.07 possess coexistence of a rombohedral-tetragonal (R-T) shape, which is indicated by the tetragonal (002) and (200), along with the rhombohedral (200) peak, as shown in Figure 3b. Here, the intensity of the tetragonal (002) peak was slowly weakened, and the rhombohedral (200) peak evidently appeared in association with the increase in antimony substitution. When x = 0.07, the piezoelectricity of the samples was greatly enhanced due to the increase of the coexistence ratio of a rombohedral-tetragonal (R-T) shape.

When the antimony x = 0.08, the rhombohedral (200) peak was appeared to be large while the tetragonal (002) peak was weakened.

The density of the samples with the antimony are shown in Figure 4. With the increased antimony content, the density of samples was slowly enhanced due to the densification of the crystal microstructure up to x = 0.07. In the composition ceramics above x = 0.07, the density was decreased due to over substitution to the KNN system. This was also because of the liquid phase firing effects of sintering aids (CuO melting point; 1020 °C, B_2O_3 melting point; 460 °C).

The k_P with the antimony are shown in Figure 5, and also the Q_m of the samples with the antimony are shown in Figure 6. The k_p increased with increasing antimony, when antimony was increased up to x = 0.07 (that is, k_p = 42.7%), and the k_p decreased with further increase above x = 0.07. The results can also illustrated the fact that the densification of the samples decreases due to the over addition of antimony, and that Q_m slowly reduced with increasing antimony content. When the content of antimony was x = 0.04, the maximum of Q_m = 80 was obtained. This perhaps indicates that the Sb^{5+} ion can enter into the B-sites of Zr^{4+} except for Nb^{5+} due to the softener effect leading to a decrease in Q_m with increasing antimony content.

(**a**) Wide Range
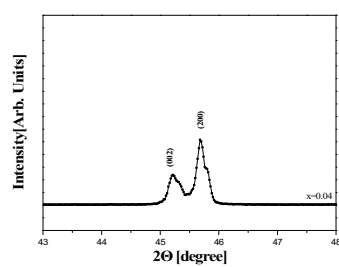
(1) x=0.04
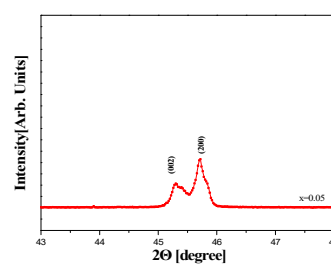
(2) x=0.05
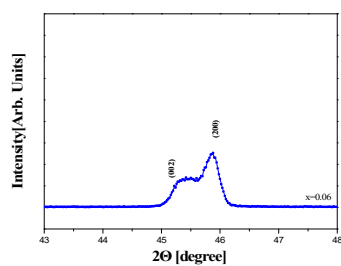
(3)x=0.06
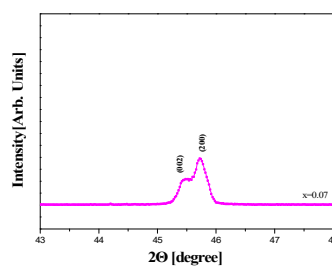
(4)x=0.07
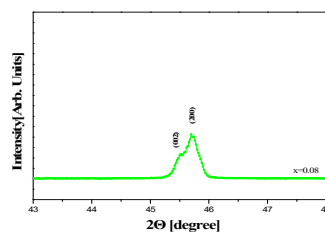
(5)x=0.08e

(**b**) Narrow Range

Figure 3. X-ray diffraction patterns of samples with the amount of antimony: (**a**) Wide Range, (**b**) Narrow Range.
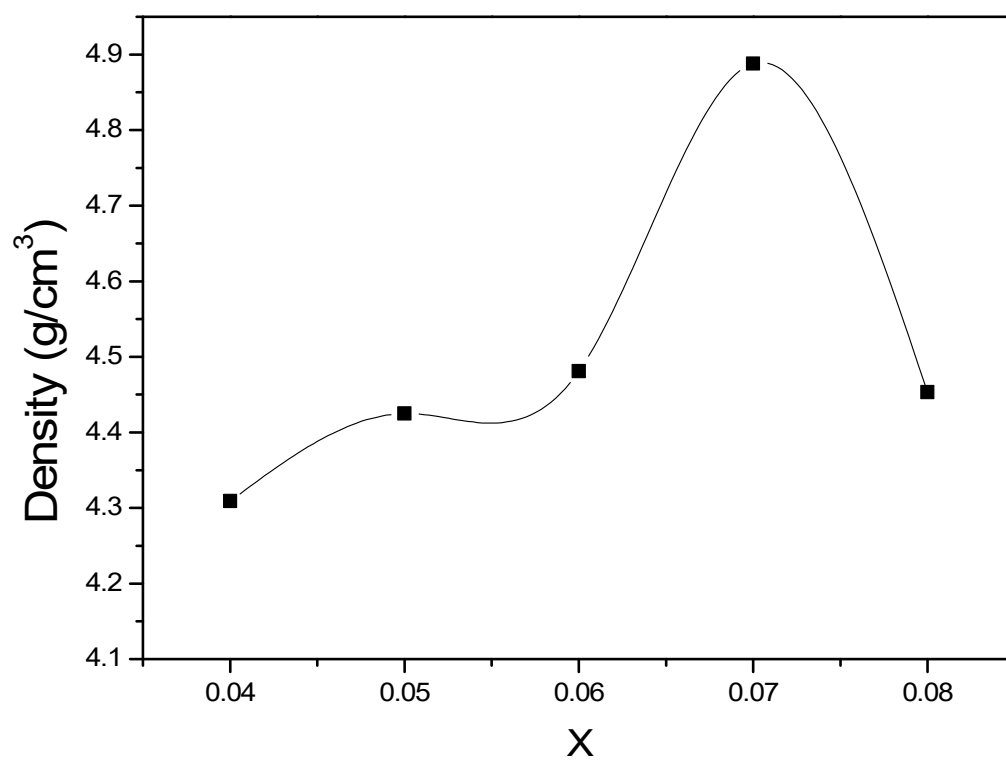
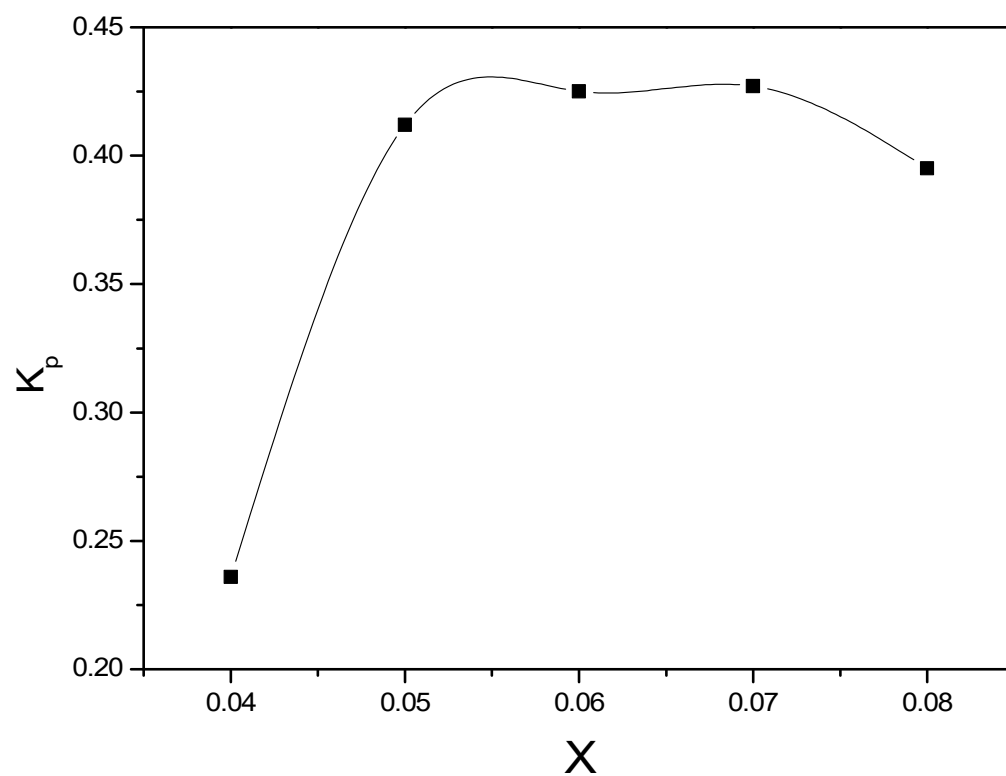**Figure 4.** Density of samples with the amount of antimony.

Figure 5. Electromechanical coupling factor (k_p) of samples with the amount of antimony.
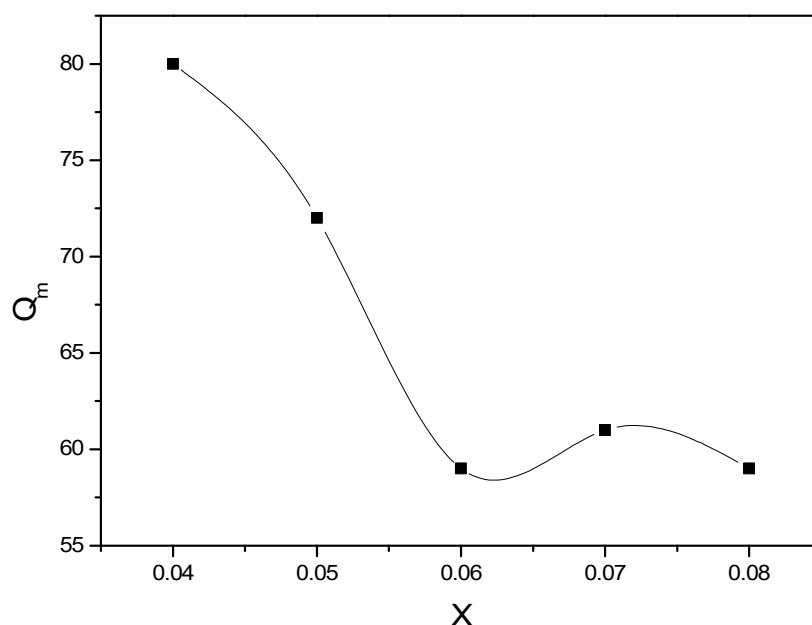
Figure 6. Mechanical quality factor (Qm) of samples with the amount of antimony.

The dielectric constant ε_r and piezoelectric constant d_{33} of samples with the antimony are shown in Figures 7 and 8, respectively. The dielectric constant ε_r of samples with the antimony increased linearly. After poling the samples as a 3 kV/mm electric field (E), the d_{33} was measured. The d_{33} was increased with the content of antimony up to x = 0.07 and then reduced above x = 0.07. In general, in order to increase the sound pressure level of the piezoelectric speaker, the highest d_{33} is required because the strain (S) is in proportion to the electric field (E). The ceramics with x = 0.07 possessed the best piezoelectricity (d_{33} = 330 pC/N, ε_r = 2521) for piezoelectric speaker application. These values were shown to be higher than d_{33} = 241 pC/N and ε_r = 1705 in our recently published paper [21,22].
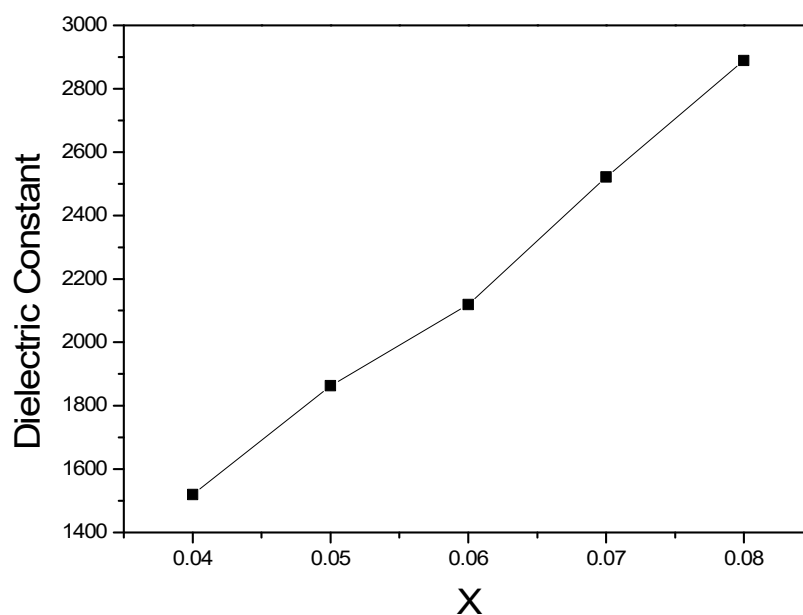

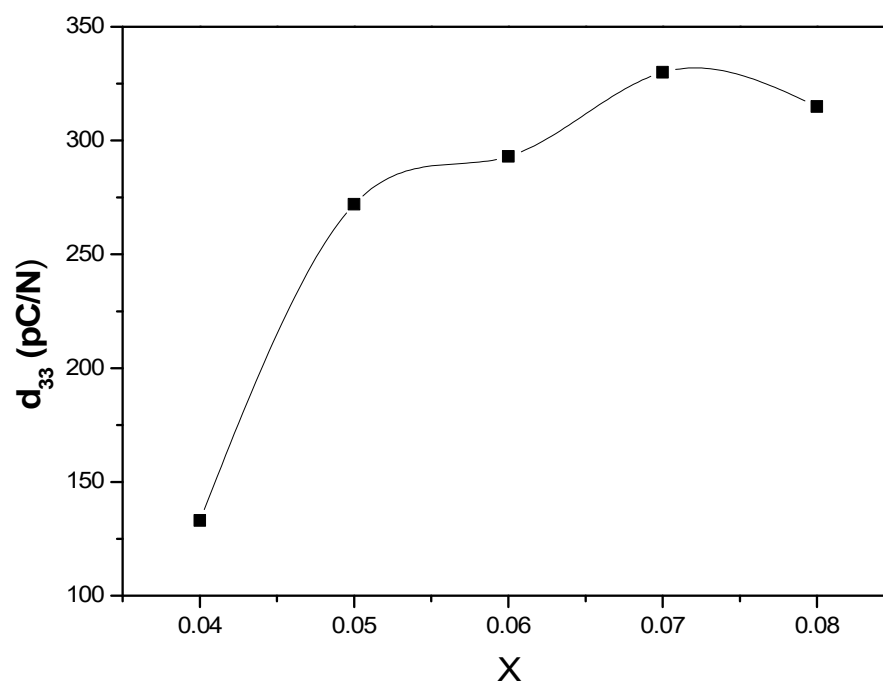**Figure 7.** Dielectric constant (ε_r) of samples with the amount of antimony.

Figure 8. Piezoelectric constant (d33) of samples with the amount of antimony.

The antimony content can enhance the sinterability of the samples together with the liquid phase formation of CuO and B_2O_3, resulting in enhancement of d_{33} and ε_r. The d_{33} of x = 0.07 specimen with electric field shown in Figure 9.
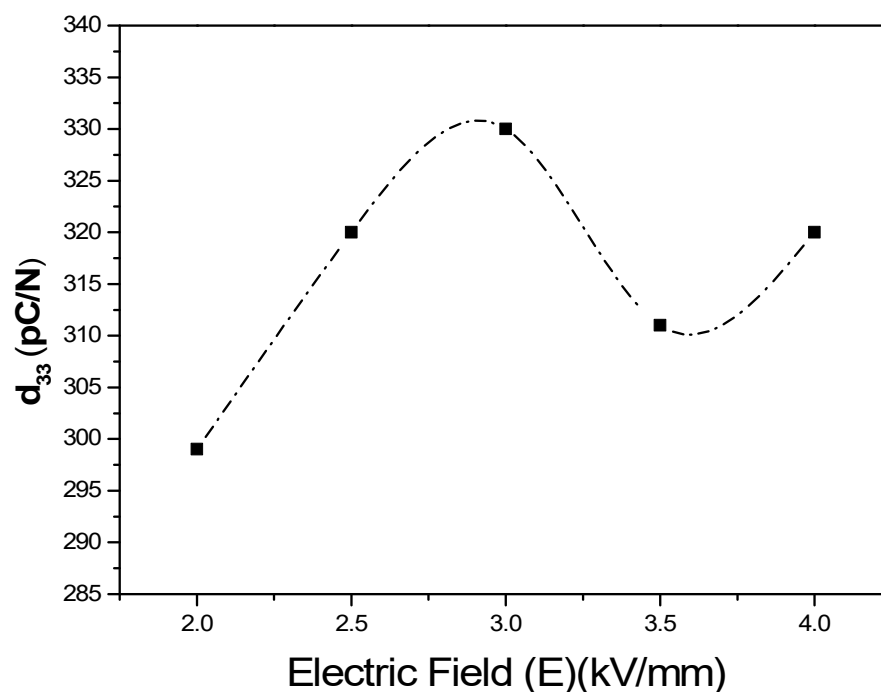

Figure 9. Piezoelectric constant (d_{33}) of x = 0.07 samples with electric field.

As the electric field (E) increased, the piezoelectric constant d_{33} increased. When the electric field (E) was 3 kV/mm, the maximum d_{33} = 330 pC/N was obtained. Thereafter, the piezoelectric constant d_{33} was decreased due to a micro-cracking phenomenon under over electric field (E) of the specimen.

The dielectric constant temperature dependence of the samples with the antimony are shown in Figure 10. Primary phase transition temperature T_{R-T} slowly increased and also the Curie temperature T_c gradually decreased according to the increase in antimony.
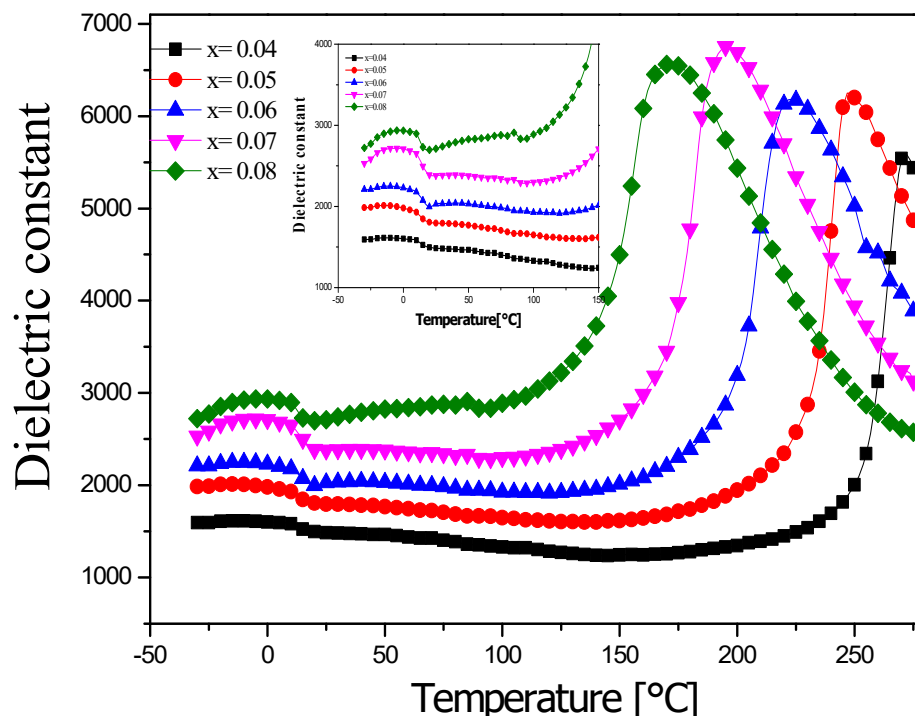

Figure 10. Temperature dependence of dielectric constant with the amount of antimony.

Physical properties of the samples with the amount of antimony are summarized in Table 1.

Table 1. Electrical properties of samples with the amount of antimony.

Sintering Temperature (°C)	X	Density (g/cm³)	k_p	Dielectric Constant	d_{33} (pC/N)	Q_m	T_c (°C)
	0.04	4.309	0.236	1520	133	80	280
	0.05	4.425	0.412	1863	272	72	250
1060	0.06	4.481	0.425	2119	293	59	225
	0.07	4.488	0.427	2521	330	61	195
	0.08	4.453	0.395	2889	315	59	170

4. Conclusions

In this experiment, the modified $(Na,K,Li)NbO_3$–$(Bi,Ba)ZrO_3$ ceramics were manufactured using CuO, B_2O_3, and ZnO as the sintering aids as a function of antimony substitution. Their crystal structure and electrical characteristics were analyzed as follows:

1. The grain size was refined as the amount of antimony increased.
2. Dielectric constant was enhanced and Curie temperature was decreased due to the content of antimony substitution.
3. With the x = 0.08 specimen, the rhombohedral (200) peak appeared. When the amount of antimony was between x = 0.04 and x = 0.07, the coexistence of the tetragonal and rhombohedral phase apparently appeared.

4. The x = 0.07 sample sintered at 1060 °C presented the best electrical characteristics: bulk density = 4.488 g/cm^3, d_{33} = 330pC/N, k_p = 0.427, Q_m = 61, and ε_r = 2521. We believe that the x = 0.07 sample is the best material for piezoelectric speakers.

References

1. Yoo, J. Excellent piezoelectric properties and high T_c in Fe_2O_3-doped PMW-PNN-PZT ceramics. *Ferroelectr. Lett. Sect.* **2018**, *45*, 1–7. [CrossRef]
2. Kim, S.; Yoo, J. PHYSICAL CHARACTERISTICS OF (1-X)(NKL)(NST) O_3-X($BA_{0.90}$ $CA_{0.1}$) ZRO_3 CERAMICS. *Trans. Electr. Electron. Mater.* **2019**, *20*, 426–430. [CrossRef]
3. Cho, S.; Jeong, Y.-H.; Yoo, J. Dielectric and piezoelectric properties of $0.97(Na_{0.52}K_{0.443}Li_{0.037})(Nb_{0.96-x}Sb_{0.04}Ta_x)O_3$-$0.03(Bi_{0.5}Na_{0.5})_{0.9}(Sr)_{0.1}ZrO_3$ ceramics for pizoelectric actuator. *Trans. Electr. Electron. Mater.* **2019**, *20*, 328. [CrossRef]
4. Yoo, J. Dielectric and piezoelectric properties of $(Na_{0.52}K_{0.443}Li_{0.037})(Nb_{0.883}Sb_{0.08}Ta_{0.037})O_3$ ceramics substituted with $(Bi_{0.5}Na_{0.5})_{0.9}(Sr)_{0.1}ZrO_3$. *Ferroelectrics* **2019**, *550*, 220–227. [CrossRef]
5. Minho, P.; Yoo, J. Piezoelectric and dielectric properties of nonstoichiometric $(Na_{0.5}K_{0.5})_{0.97}(Nb_{0.90}Ta_{0.1})O_3$ ceramics doped with MnO_2. *J. Electron. Mater.* **2012**, *41*, 3095–3099.
6. Zhou, C.; Zhang, J.; Yao, W.; Liu, D.; Su, W. Highly temperature-stable piezoelectric properties of $0.96(K_{0.48}Na_{0.52})(Nb_{0.96}Sb_{0.04})O_3$-$0.03BaZrO_3$-$0.01(Bi_{0.50}Na_{0.50})ZrO_3$ ceramic in common usage temperature range. *Scr. Mater.* **2019**, *162*, 86. [CrossRef]
7. Zhang, B.Y.; Wu, J.G.; Cheng, X.J.; Wang, X.P.; Xiao, D.Q.; Zhu, J.G.; Wang, X.J.; Lou, X.J. Large d_{33} in (K,Na)(Nb,Ta,Sb)O_3-(Bi,Na,K)ZrO_3 lead-free ceramics. *J. Mater. Chem. A* **2014**, *2*, 4122–4126.
8. Zheng, J.G.; Wu, Q.; Chen, D.; Xiao, Q.; Zhu, J.G. Composition-driven phaseboundary and piezoelectricity in potassium_sodium niobate-based ceramics. *ACS Appl. Mater. Interfaces* **2015**, *7*, 20332–20341. [CrossRef] [PubMed]
9. Rubio-Marcos, F.; Lopez-Juarez, R.; Rojas-Hernandez, R.E.; del Campo, A.; Razo-Perez, N.; Fernandez, J.F. Lead-free piezo ceramics: Revealing the role of the rhombohedral-tetragonal phase coexistence in enhancement of the piezoelectric properties. *ACS Appl. Mater. Interfaces* **2015**, *7*, 23080–23088. [CrossRef]
10. Tao, H.; Wu, J.G.; Wang, H. Modification of strain and piezoelectricity in (K,Na)NbO_3–(Bi,Na)HfO_3 lead-free ceramics with high Curie temperature. *J. Alloys Compd.* **2016**, *684*, 217–233. [CrossRef]
11. Xu, K.; Li, J.; Lv, X.; Wu, J.G.; Zhang, X.X.; Xiao, D.Q.; Zhu, J.G. Superior piezoelectric properties in potassium sodium niobate lead-free ceramics. *Adv. Mater.* **2016**, *28*, 8519–8523. [CrossRef]
12. Wu, B.; Wu, H.J.; Wu, J.G.; Xiao, D.Q.; Zhu, J.G.; Pennycook, S.J. Giant piezoelectricity and high curie temperature in nanostructured alkali niobate lead-free piezo ceramics through phase coexistence. *J. Am. Chem. Soc.* **2016**, *138*, 15459. [CrossRef]
13. Xiang, R.; Wu, J. Contribution of $Bi_{0.5}Na_{0.5}ZrO_3$ on phase boundary and piezoelectricityin $K_{0.48}Na_{0.52}Nb_{0.96}Sb_{0.04}O_3$-$Bi_{0.5}Na_{0.5}SnO_3$-$xBi_{0.5}Na_{0.5}ZrO_3$ ternary ceramics ceramics. *J. Alloys Compd.* **2020**, *820*, 153411.
14. Gou, Q.; Zhu, J.; Wu, J.; Li, F.; Jiang, L.; Xiao, D. Microstructure and electrical properties of $(1-x)K_{0.5}Na_{0.5}NbO_3$-$xBi_{0.5}Na_{0.5}Zr_{0.85}Sn_{0.15}O_3$ lead-free ceramics. *J. Alloys Compd.* **2018**, *730*, 311–317. [CrossRef]
15. Jaffe, B.; Cook, W.R.; Jaffe, H. *Piezoelectric Ceramics*; Academic Press: Cambridge, MA, USA, 1971.
16. Yoo, J. Effect of sintering temperature on the dielectric and piezoelectric properties of $(Na_{0.525}K_{0.443}Li_{0.037})(Nb_{0.883}Sb_{0.08}Ta_{0.037})O_3$ Pb-free ceramics for actuator. *Ferroelectrics* **2017**, *507*, 12. [CrossRef]
17. Noh, J.; Yoo, J. Dielectric and piezoelectric properties of KCT added $(Li_{0.02}(Na_{0.56}K0.46)0.98(Nb_{0.81}Ta_{0.15}Sb_{0.04})O_3$ ceramics. *J. Electroceram.* **2013**, *30*, 139–144. [CrossRef]
18. Yoo, J.; Lee, J. The effects of MnO_2 addition on the physical properties of $Pb(Ni_{1/3}Nb_{2/3})O_3$-$Pb(Zr,Ti)O_3$-$Pb(Mg_{1/2}W_{1/2})O_3$-$BiFeO_3$ ceramics. *Crystals* **2021**, *11*, 269. [CrossRef]
19. Zhou, C.; Zhang, J.; Yao, W.; Liu, D.; He, G. Remarkably strong piezoelectricity, rhombohedral-orthorhombic-tetragonal phase coexistence and domain structure of (K,Na)(Nb,Sb)O_3-(Bi,Na)ZrO_3-$BaZrO_3$ ceramics. *J. Alloys Compd.* **2020**, *820*, 153411. [CrossRef]
20. Yoo, J.; Lee, J. Microstructure and piezoelectricity of (Na,K,Li)(Nb,Sb)O_3–(Bi,Na)(Sr)ZrO_3–$BaZrO_3$ ceramics. *Crystals* **2020**, *10*, 868. [CrossRef]
21. Zhang, B.; Wu, J.; Cheng, X.; Wang, X.; Xiao, D.; Zhu, J.; Wang, X.; Lou, X. Lead-free piezoelectrics based on potassium–sodium niobate with giant d_{33}. *ACS Appl. Mater. Interfaces* **2013**, *5*, 7718–7725. [CrossRef]
22. Yoo, J.; Lee, Y.W.; Lee, J. Dielectric and piezoelectric properties of $0.965(Na_{0.5}K_{0.5})_{0.97}Li_{0.03}(Nb_{0.96}Sb_{0.04})O_3$–$0.035(Bi_{0.5}Na_{0.5})_{0.9}(Sr)_{0.1}ZrO_3$ ceramics with CuO addition. *Ferroelectrics* **2021**, *572*, 51. [CrossRef]